EPR and DFT Studies of the Structure of Phosphinyl Radicals Complexed by a Pentacarbonyl Transition Metal

Bassirou Ndiaye,[†] Shrinivasa Bhat,[†] Abdelaziz Jouaiti,[†] Théo Berclaz,[†] Gérald Bernardinelli,[‡] and Michel Geoffroy*[,†]

Department of Physical Chemistry, 30 Quai Ernest Ansermet, University of Geneva, 1211 Geneva 4, Switzerland, and Laboratory of X-ray Crystallography, 24 Quai Ernest Ansermet, University of Geneva, 1211 Geneva 4, Switzerland

Received: March 30, 2006; In Final Form: June 9, 2006

Paramagnetic complexes $M(CO)_5P(C_6H_5)_2$, with M = Cr, Mo, W, have been trapped in irradiated crystals of $M(CO)_5P(C_6H_5)_3$ (M = Cr, Mo, W) and $M(CO)_5PH(C_6H_5)_2$ (M = Cr, W) and studied by EPR. The radiolytic scission of a P−C or a P−H bond, responsible for the formation of $M(CO)_5P(C_6H_5)_2$, is consistent with both the number of EPR sites and the crystal structures. The *g* and ^{31}P hyperfine tensors measured for $M(CO)_5P(C_6H_5)_2$ present some of the characteristics expected for the diphenylphosphinyl radical. However, compared to $Ph_2P^{\bullet}$, the ^{31}P isotropic coupling is larger, the dipolar coupling is smaller, and for Mo and W compounds, the *g*-anisotropy is more pronounced. These properties are well predicted by DFT calculations. In the optimized structures of $M(CO)_5P(C_6H_5)_2$ (M = Cr, Mo, W), the unpaired electron is mainly confined in a phosphorus p-orbital, which conjugates with the metal d_{xz} orbital. The trapped species can be described as a transition metal-coordinated phosphinyl radical.

1. Introduction

During the past five years many studies have invoked or confirmed the participation of metal-containing radicals to several mechanisms particularly important in modern chemistry. This is especially the case for metal-mediated oxygenation processes encountered in the synthesis of fine chemicals and in various areas of biochemistry (e.g., metalloenzymes).[1,2] The crucial point in the description of an organometallic radical concerns the localization of the unpaired electron. In most cases, the chemical properties of the complex indicate that the transition metal contains 17 or 19 valence electrons, suggesting that the spin delocalization on the ligand is practically negligible. In some few cases ("Ligand Non-innocence"[3]), however, all the metal valence bond electrons remain paired, and the chemical behavior of the complex is similar to that of an organic radical.[4−7] This type of structure has been reported for $[R_3Ir(MeCN)(ethene)]^{2+}$ whose structure is better described by $Ir^{III}-CH_2-CH_2^{\bullet}$ than by $Ir^{II}(CH_2{=}CH_2)$.[4] Very recently, the first stable aminyl radical metal complex has been reported by Grützmacher.[8] In phosphorus chemistry several complexes have been reported in which the unpaired electron lies on the ligand; they generally result, however, from the reduction of a system containing an electron π acceptor ligand, like a phosphinine or a phosphaalkene, able to stabilize the radical anion.[9] In the present study, our purpose is to get information about the structure of system **A** composed of a neutral phosphorus-centered radical $^{\bullet}PR_2$, a phosphinyl radical, bound to a transition metal moiety containing *n* d-electrons. Two other limiting structures can, a priori, be envisaged for such systems (Scheme 1).

SCHEME 1

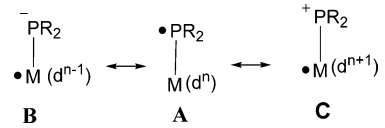

In **B**, a phosphido-type ligand is linked to a metal containing $(n - 1)$ d-electrons. Phosphido complexes are well documented,[10] and their formation through the scission of the P−H bond of a complexed secondary phosphine has recently be used in the context of enantioselective catalysis.[11] In **C**, the metal contains $(n + 1)$ d-electrons while the ligand is formally a phosphenium group, a group 15 carbenoid. Structure and reactivity of carbenoids and phosphheniums continue to be objects of current interest[12] as well as the chemistry of transition metal complexes containing a phosphenium ligand.[13]

Due to their reaction-intermediate nature, it is difficult to get information about the structure of transient metalated radicals. Liquid solution EPR is well suited to their identification but a part of the structural information is lost due to the averaging of the *g* and hyperfine tensors. There is no doubt that the most efficient method is to trap the metalated radical in an oriented matrix and to compare the resulting EPR tensors with those predicted by DFT calculations for the wanted species. The difficulty lies in the production of the transition metal-complexed radical. In the present study, we have tried to generate these species by exposing single crystals of phosphines complexed by metal pentacarbonyls to ionizing radiation. At room temperature, the diffusion of a group R resulting from the homolytic scission of a P−R bond is expected to be sufficiently efficient to lead to the trapping of $M(CO)_5PR_2$. The corresponding **A** structure (Scheme 1) is represented in Chart 1. In this work, EPR measurements and DFT calculations have been performed on complexes where the metal is Cr, Mo, or W and where the organic groups bound to the phosphorus atom are phenyl groups.

* Address correspondence to this author. Phone: (41) 22-379-65-52. Fax: (41) 22-379-61-03. E-mail: michel.geoffroy@chiphy.unige.ch.
[†] Department of Physical Chemistry.
[‡] Laboratory of X-ray Crystallography.

10.1021/jp061960w CCC: $33.50
Published on Web 07/19/2006

TABLE 1: Summary of Crystal Data, Intensity Measurement, and Structure Refinement

	$Cr(CO)_5P(C_6H_5)_3$	$Cr(CO)_5P(H)(C_6H_5)_2$	$W(CO)_5P(H)(C_6H_5)_2$
formula	$C_{23}H_{15}CrO_5P$	$C_{17}H_{11}CrO_5P$	$C_{17}H_{11}O_5PW$
M_r	454.3	378.2	510.1
crystal size (mm^3)	0.25 × 0.26 × 0.30	0.14 × 0.22 × 0.25	0.22 × 0.22 × 0.15
diffractometer	Nonius CAD4	Stoe IPDS	Stoe STADI4
temp (K)	293	200	293
crystal system	monoclinic	monoclinic	monoclinic
space group	*I*2/*a*	$P2_1/c$	$P2_1/c$
a (Å)	11.247(2)	13.2726(9)	13.352(3)
b (Å)	15.014(2)	15.6622(9)	15.931(3)
c (Å)	25.636(5)	8.6557(6)	8.7070(10)
β (deg)	102.346(8)	106.297(11)	105.980(10)
V ($Å^3$)	4228.8(13)	1727.0(2)	1780.5(6)
Z	8	4	4
D_x ($g\cdot cm^{-3}$)	1.427	1.455	1.903
μ(Mo Kα) (mm^{-1})	0.648	0.780	6.5992
T_{min}, T_{max}	0.8253, 0.8857	0.8508, 0.9117	0.2455, 0.4316
$((\sin\theta)/\lambda)_{max}$ ($Å^{-1}$)	0.595	0.615	0.550
no. of measured reflcns	3969	13792	2561
no. of independent reflcns	3696	3355	2443
no. of observed reflcns	2804	2161	1964
R_{int}	0.029	0.040	0.022
criterion for observed	$\|F_o\| > 4\sigma(F_o)$	$\|F_o\| > 4\sigma(F_o)$	$\|F_o\| > 4\sigma(F_o)$
refinement (on *F*)	full-matrix	full-matrix	full-matrix
no. of parameters	317	250	250
weighting scheme p^a	0.0001	0.0002	0.0
max Δ/σ	0.001	0.0004	0.006
max and min $\Delta\rho$ ($e\cdot Å^{-3}$)	0.39, −0.34	0.32, −0.29	0.98, −0.79
S^b (all data)	1.46(2)	1.34(2)	1.78(2)
R,^{c} ωR^d	0.041, 0.038	0.035, 0.038	0.031, 0.020

^{a} $\omega = 1/[\sigma^2(F_o) + p(F_o)^2]$. ^{b} $S = [\sum\{((F_o - F_c)/\sigma(F_o))^2\}/(N_{ref} - N_{var})]^{1/2}$. ^{c} $R = \sum||F_o| - |F_c||/\sum|F_o|$. ^{d} $\omega R = [\sum(\omega|F_o| - |F_c|)^2/\sum\omega|F_o|^2]^{1/2}$.

CHART 1

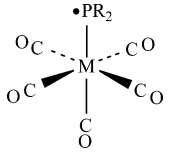

2. Experimental Section

Compounds. Syntheses of $Cr(CO)_5P(C_6H_5)_3$, $Mo(CO)_5P(C_6H_5)_3$, and $Mo(CO)_5P(C_6H_5)_3$ have been published.[14] The syntheses of $Cr(CO)_5P(H)(C_6H_5)_2$ and $W(CO)_5P(H)(C_6H_5)_2$ have been carried out by adapting the method reported by Mathey et al. for $W(CO)_5P(C_6H_5)H_2$.[15]

Crystal Structure. A Summary of crystal data, intensity measurement, and structure refinement is reported in Table 1. For each crystal structure, hydrogen atoms were observed and refined with a fixed value of their isotropic displacement parameters. CCDC 600424 to 600426 contains the supplementary crystallographic data for this paper. These data can be obtained free of charge via www.ccdc.cam.ac.uk/conts/retrieving.html (or from the Cambridge Crystallographic Data Centre, 12 Union Road, Cambridge CB2 1EZ, UK; fax (+ 44) 1223-336-033; or deposit@ccdc.cam.ac.uk).

Single-Crystal EPR Measurements. EPR spectra were recorded on a Bruker spectrometer (X-band). The angular variations of the EPR signals were recorded in the three reference planes of a Cartesian referential XYZ oriented with respect to the crystallographic axes as follows: for $Cr(CO)_5P(C_6H_5)_3$ X//a, Y//b, Z//c*; for $Cr(CO)_5P(H)(C_6H_5)_2$ X//c*, Y//b, Z//c; for $Mo(CO)_5P(C_6H_5)_3$ X//a*, Y//c*; for $W(CO)_5P(C_6H_5)_3$ Y//b* and Z//a; for $W(CO)_5P(H)(C_6H_5)$ X (//c), Y//b, Z//a*. The EPR tensors were determined by using an optimization program that compares the positions of the signals with the resonance field positions calculated by using second-order perturbation theory.[16] The angular variations of the EPR signals obtained with the five crystals are given in the Supporting Information.

Calculations. DFT calculations were performed with the Gaussian 03 package.[17] All the geometries were optimized by using the hybrid functional B3LYP,[18,19] the standard 6-31G-(d,p) basis set for H, C, O, and P, and the basis set SBKJC[20a,21] developed by Stevens et al. for the transition metal. The SBKJC set[20] uses Relativistic Compact Effective Potentials and efficient, share-exponent basis sets for the third-, fourth-, and fifth-row atoms. In this approach, outermost $(n + 1)$s orbitals (where *n* is the principal quantum number), the partially occupied *n*d orbitals, as well as the *n*s and *n*p orbitals are considered to be part of the valence space. For transition metals the basis functions consist of double-ζ quality sp basis sets (contraction 4,1) and triple-ζ d basis sets (contraction 4,1,1 for third row; 3,1,1 for fourth and fifth rows), and the outer s and p primitives are contracted 2,1 for Cr and Mo and 1,1 for W. Two sets of calculations were performed for the prediction of the *g* and hyperfine tensors. The first one used the IGLO-III basis set[21,22] (Invariant Gauge Localized Orbitals) for H, C, O, and P atoms while the second one used the TZVP basis set.[23] In IGLO-III, the Gaussian-type functions, developed by Kutzelnig and intended for computing magnetic properties, were derived from Double-ζ Huzinaga functions to which a double set of polarization functions was added. This basis set consists of the following contractions: (6s,2p)/[4s,2p] for H, (11s,7p,2d)/[7s,6p,2d] for first-row atoms, and (12s,8p,3d)/[8s,7p,3d] for second-row atoms. The TZVP basis set[21,23a] consists of the contractions (5s,-1p)/[3s,1p] for H, (10s,6p,1d)/[4s,3p,1d] for C and O, and (13s,-9p,1d)/[5s,4p,1d] for P.

Minima were characterized with harmonic frequency calculations (no imaginary frequencies). Molecular orbitals were represented using the GaussView program.[24]

Many studies have been devoted to the calculation of EPR properties.[25] The isotropic part (Fermi contact interaction) and

TABLE 2: Geometrical Parameters[a] Determined from Crystal Structures

	M−P	M−C_{axial}	$(M-C_{equ})_{av}$	P−M-C_{axial}	M−P−R (av value)	ξ^b			φ^c
$Cr(CO)_5P(C_6H_5)_3$[d]	2.405(1)	1.870(3)	1.897	177.7(1)	115.9	45.1	42.2	45.5	102.3
$Cr(CO)_5P(H)(C_6H_5)_2$[d]	2.374(1)	1.868(3)	1.900	176.7(1)	117.5	41.4	47.5	50.8	100.0
$Mo(CO)_5P(C_6H_5)_3$[e]	2.560(1)	1.995(3)	2.046	174.4(1)	115.6	43.6	40.9	47.4	102.6
$W(CO)_5P(C_6H_5)_3$[f]	2.545(1)	2.006(5)	2.033	174.2(2)	115.4	40.8	43.3	46.9	102.9
$W(CO)_5P(H)(C_6H_5)_2$[d]	2.508(2)	1.968(9)	2.012	176.0(2)	116.6	39.4	45.7	50.4	101.6

[a] Distances in Å, angles in deg. [b] Angle formed by the P−M bond with the normals to the CPC or CPH planes. [c] Average value of the CPC and CPH bond angles. [d] This work. [e] Reference 27. [f] Reference 28.

the anisotropic part (electron−nuclear dipole interaction) of the hyperfine interaction at a nucleus N can be expressed as

$$A_{iso} = (8\pi/3)g\beta g_N\beta_N \sum^{\mu,\nu} \mathbf{P}_{\mu\nu}^{\alpha-\beta}\langle\phi_\mu|\delta(\vec{r}_N)|\phi_\nu\rangle$$

$$\tau_{pq}^N = -g\beta g_N\beta_N \sum^{\mu,\nu} \mathbf{P}_{\mu\nu}^{\alpha-\beta}\langle\phi_\mu|(r^2\delta_{pq} - 3pq)r^{-5}|\phi_\nu\rangle$$

respectively. The molecular orbitals are defined as linear combinations of atomic orbitals ϕ_μ, $\mathbf{P}_{\mu\nu}^{\alpha-\beta}$ represents an element of the one-electron spin density matrix, and *pq* the spatial coordinates *x*,*y*,*z* relative to the nucleus N.

Calculation of the elements of the *g*-tensor requires evaluating four contributions.[26]

$$g_{rs} = g_e\delta_{rs} + \Delta g_{[RMC]}\delta_{rs} + \Delta g_{rs[GC]} + \Delta g_{rs[OZ/SOC]}$$

The first term corresponds to the value of the free electron; the second one is due to the relativistic mass correction to the kinetic energy. The diamagnetic correction $\Delta g_{[GC]}$ involves the effective spin−orbit coupling interaction ξ(A,i) of the electron i at the nucleus A (with $\xi(r_{iA}) = \alpha^2 Z_{eff}^A/2|r_i - R_A|^3$, where Z_{eff}^A is an effective nuclear charge for atom A at position R_A). $\Delta g_{[OZ/SOC]}$ arises as a cross term between the orbital Zeeman ($H_{OZ} = \beta\Sigma B\, l(i)$) and spin−orbit coupling ($H_{SOC} = \sum\xi(r_{iA})l_A(i)s(i)$) operators. $l(i)$ is the angular momentum operator of the *i*th electron relative to the chosen gauge origin and $s(i)$ is the spin operator for this electron.

3. Results

3.1. Crystal Structures. The crystal structures of three of the five diamagnetic precursors, $M(CO)_5P(C_6H_5)_3$, M = Mo,[27] W,[28] and Cr,[29] are isostructural, and are available in the literature.[30] However, for M = Cr, the crystals used in our EPR study were found to grow in another crystal system; the corresponding structure is reported below. Both structures of isostructural compounds $Cr(CO)_5P(H)(C_6H_5)_2$ and $W(CO)_5P(H)(C_6H_5)_2$ were also determined in the present study. An ORTEP view of the crystal structure of $Cr(CO)_5P(H)(C_6H_5)_2$ is given in Figure 1.

The principal geometrical parameters determined from the crystal structures are given in Table 2. The five complexes adopt the classical square-planar bipyramid structure with a M−C_{axial} distance slightly shorter than the M−$C_{equatorial}$ bond lengths. The ξ angles formed by the normal to the RPR planes and the M−P bond indicate that the coordination of the phosphorus atom is not too far from tetrahedral (for a pure tetrahedron $\xi = 35.26°$). As shown by the sum of the CPC (and CPH) angles, which is between 300°and 309°, the pyramidality of the phosphine moiety is not very affected by the coordination to the metal atom (for the isolated triphenylphosphine $\sum R_iPR_j = 308.9°$).[31]

3.2. EPR Measurements. The spectra obtained at room temperature with the five irradiated crystals presented all the same features: an anisotropic coupling with a spin $^1/_2$ nucleus—certainly ^{31}P—and a rather pronounced *g* anisotropy. An example of a spectrum obtained with a crystal of $Cr(CO)_5P(C_6H_5)_3$ is shown in Figure 2 (signals R).

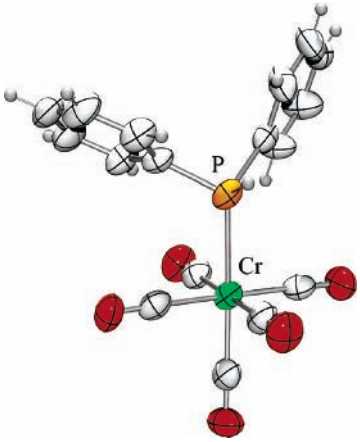

Figure 1. Ortep view of the crystal structure of $Cr(CO)_5P(H)(C_6H_5)_2$. Ellipsoids are represented with 50% probability level.

The EPR tensors determined after analysis of the angular dependences[32] are shown in Table 3 together with the values previously reported for the isolated $P(C_6H_5)_2$ radical.[33]

For all species, the symmetry of the ^{31}P hyperfine tensor is axial (with the largest eigenvalue $T_{max} = T_{||}$) and g_{min}, close to the free electron value, is oriented in the vicinity of the ^{31}P-$T_{||}$ vector. Moreover, as shown in Table 4, decomposition into isotropic and anisotropic ^{31}P coupling constants clearly indicates that a large amount of the unpaired electron resides in a phosphorus p-orbital. Comparison with atomic hyperfine constants[34] leads to a crude estimation of the s and p characters of the spin-containing phosphorus orbital $\rho_s \cong 0.035$ and $\rho_p \cong 0.55$. These properties are similar to those expected for a phosphinyl radical[33] and suggest a homolytic scission of a phosphine bond. We will therefore examine if this interpretation is consistent with the properties of the crystals.

After rupture of a P−C bond in $M(CO)_5P(C_6H_5)_3$, the resulting radical relaxes to its minimum energy conformation; this process is likely to be hindered by the environment of the remaining phenyl rings. As shown by the crystal structure, in each compound the environments of the three phenyl rings are slightly different. This is clearly seen from the three different ξ values measured in each complex (Table 2) and from the P−C_{phenyl} bonds which are differently oriented with regard to the metal−carbon bonds of the equatorial plane. For example, in $Mo(CO)_5P(C_6H_5)_3$ (where C1, C2, C3, and C4 form the equatorial plane), the P−C8 bond lies in the C3−Mo−C4 bisector while the bonds P−C6 and P−C7 make dihedral angles of 15° with Mo−C1 and Mo−C2, respectively. Due to these differences in the orientations of the phenyl rings, the final structure of the trapped radical is expected to be slightly dependent upon which of the three P−C bonds has been broken.

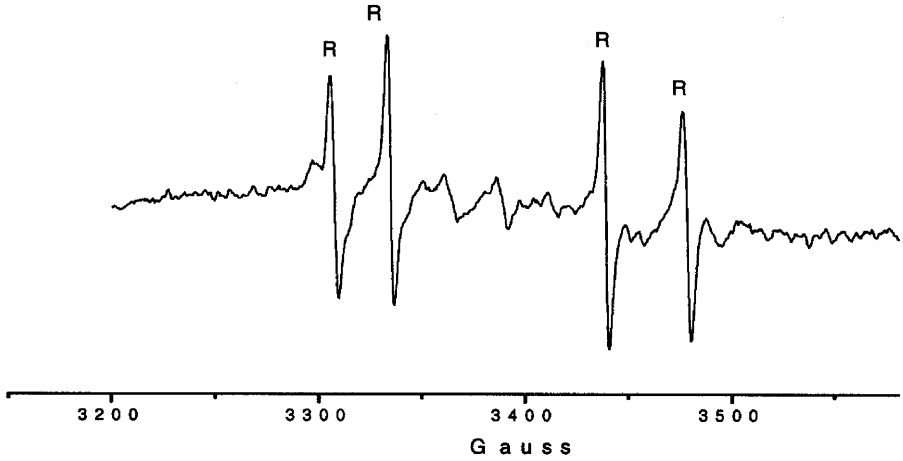

Figure 2. Example of an EPR spectrum obtained with an X irradiated single crystal of $Cr(CO)_5P(C_6H_5)_3$.

TABLE 3: Experimental EPR Tensors

crystal	*g*-tensor principal values	(^{31}P) coupling tensor **T** principal values (MHz)	eigenvector ^{31}P-T_{max}	angle (g_{min}, T_{max})
$Cr(CO)_5P(C_6H_5)_3$	2.001, 2.006, 2.012	239, 248, 869	±0.3493, −0.8689, 0.3505[a]	5
$Cr(CO)_5P(H)(C_6H_5)_2$	2.002, 2.007, 2.011	274, 292, 934	−0.2039, ±0.5417, 0.8154[a]	8
$Mo(CO)_5P(C_6H_5)_3$[b]	1.999, 2.008, 2.018	185, 193, 846	−0.1525, −0.4692, 0.8698	9
	2.003, 2.009, 2.016	187, 240, 830	0.3851, −0.9211, −0.0556	12
	2.001, 2.009, 2.014	187, 183, 837	0.9834, 0.1798, −0.0207	9
$W(CO)_5P(C_6H_5)_3$[b]	1.994, 2.018, 2.030	203, 216, 849	−0.5997, 0.0963, −0.7944	10
	2.000, 2.018, 2.023	194, 190, 837	−0.2103, 0.9762, −0.0522	12
	2.004, 2.018, 2.030	220, 222, 839	0.8928, 0.4094, −0.1878	20
$W(CO)_5P(H)(C_6H_5)_2$	2.007, 2.025, 2.016	259, 305, 932	0.2303, ±0.5136, 0.8265[a]	15
$P(C_6H_5)_2$[c]	2.0024, 2.0052, 2.0124	20, 20, 740		

[a] Two orientations in accord with the crystal structure. [b] Three sets of tensors are obtained consistent with the homolytic scission of three P−C bonds. [c] Reference 33.

TABLE 4: Experimental Isotropic and Anisotropic ^{31}P Coupling Constants (MHz) of Complexed Phosphinyl Radicals

paramagnetic species (irradiated crystal)	(^{31}P)A_{iso}	(^{31}P)-τ_{aniso}			phosphorus spin densities ρ_s	phosphorus spin densities ρ_p
$Cr(CO)_5P(C_6H_5)_2$						
($Cr(CO)_5P(C_6H_5)_3$)	452	−213	−204	417	0.03	0.57
($Cr(CO)_5P(H)(C_6H_5)_2$)	500	−226	−208	434	0.04	0.59
$Mo(CO)_5P(C_6H_5)_2$.						
($Mo(CO)_5P(C_6H_5)_3$)	408	−223	−215	438	0.03	0.60
	419	−232	−179	411	0.03	0.56
	402	−215	−219	434	0.03	0.59
$W(CO)_5P(C_6H_5)_2$						
($W(CO)_5P(C_6H_5)_3$)	423	−219	−207	426	0.03	0.58
	407	−217	−213	430	0.03	0.59
	427	−207	−205	412	0.03	0.56
($W(CO)_5P(H)(C_6H_5)_2$)	499	−239	−194	433	0.04	0.59
$P(C_6H_5)_2$[a]	260	−240	−240	480		

[a] Reference 33.

This explains the three sets of tensors obtained for $Mo(CO)_5P(C_6H_5)_3$ and for $W(CO)_5P(C_6H_5)_3$. For $Cr(CO)_5P(C_6H_5)_3$, curiously, only one P−C bond undergoes a homolytic scission—such a selection in the bond cleavage is tentatively attributed to crystal packing. For $Cr(CO)_5P(H)(C_6H_5)_2$ and $W(CO)_5P(H)(C_6H_5)$, the favored diffusion of a hydrogen atom leads to the cleavage of the P−H bond only; the two orientations observed for the trapped radical are merely due to the monoclinic symmetry of the crystal.

3.3. DFT Calculations. *3.3.1. Diphenylphosphinyl Radical.* Preliminary calculations were devoted to the structure of the phosphinyl radical $Ph_2P^{\bullet}$. Its geometry was optimized and the *g* and ^{31}P hyperfine tensors were calculated. These tensors will be reported in Table 6. A representation of the SOMO of $Ph_2P^{\bullet}$ is shown in Figure 3.

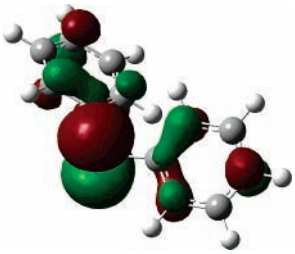

Figure 3. SOMO for the isolated $P(C_6H_5)_2$ radical.

As expected, the unpaired electron is localized in a phosphorus p-orbital oriented perpendicular to the RPR plane. The g_{min} and ^{31}P-$T_{||}$ components are aligned along this orbital direction. The normals to the phenyl rings form an angle of 51°.

3.3.2. Complexed Phosphinyl Radicals. The optimized parameters of complexed phosphinyl radicals are reported in Table 5. The ^{31}P isotropic and anisotropic coupling constants as well as the *g*-tensors calculated for the various metalated phosphinyl species are reported in Table 6, together with the corresponding values calculated for the isolated $P(C_6H_5)_2$ radical. The IGLO-III and TZVP basis sets lead to rather similar values

4. Discussion

Although the EPR tensors of the paramagnetic species trapped in the crystal matrices of pentacarbonylmetal complexes (see Tables 3 and 4) present several similarities with those expected for a phosphinyl radical (e.g., axiality of the *g* and ^{31}P hyperfine tensors, relative orientation of these tensors), these tensors differ

TABLE 5: Optimized Geometries[a] for Metalated Phosphinyl Radicals

	M−P	M−C_{axial}	$(M-C_{equ})_{ave}$	P−M−C_{axial}	M−P−R	ξ^b	φ^c
$Cr(CO)_5PPh_2$	2.389	1.900	1.924	180	125.5[d]	77	106.98
$Mo(CO)_5PPh_2$	2.527	2.041	2.077	180	126.2	90	107.49
$W(CO)_5PPh_2$	2.514	2.024	2.063	180	126.1	90	107.7

[a] Distances in Å, angles in degree, geometry optimized with 6-31G(d,p) for C, O, P, H and the SBKJC basis set for the transition metal. [b] ξ: angle between the normal to the RPR′ plane and the M−P bond. [c] CPC value. [d] The two CrPC angles were found to be slightly different: 124° and 127°.

TABLE 6: DFT Calculated EPR Parameters for Metalated Phosphinyl Radicals[a]

radical species		*g*-tensor		$(^{31}P)A_{iso}$ (MHz)	(^{31}P)-τ_{aniso} (MHz)			angle (g_{min}, τ_{max}) (deg)	phosphorus atomic spin density
$Cr(CO)_5P(C_6H_5)_2$	1.9999	2.0056	2.0113[a]	312[a]	−223	−221	444[a]	6.4	0.77
	1.9999	2.0059	2.0119[b]	320[b]	−228	−226	454[b]	5.7	0.77
$Mo(CO)_5P(C_6H_5)_2$.	2.0005	2.0088	2.0148[a]	281[a]	−229	−224	453[a]	0.5	0.78
	2.0006	2.0092	2.0154[b]	290[b]	−234	−230	463[b]	0.5	0.77
$W(CO)_5P(C_6H_5)_2$	1.9986	2.0205	2.0221[a]	281[a]	−223	−219	442[a]	15.7	0.75
	1.9989	2.0211	2.0225[b]	293[b]	−229	−225	454[b]	6.5	0.74
$P(C_6H_5)_2$	2.0022	2.0047	2.0130[a]	164[a]	−268	−250	519[a]	5.0	0.84
	2.0022	2.0050	2.0140[b]	190[b]	−271	−255	527[b]	2.0	0.82

[a] Calculated with IGLO-III for C, O, P, H and the SBKJC basis set for the transition metal at the geometry optimized with 6-31G(d, p) for C, O, P, H and SBKJC for the transition metal. [b] By using the TZVP basis set for C, O, P, H for the calculation of properties.

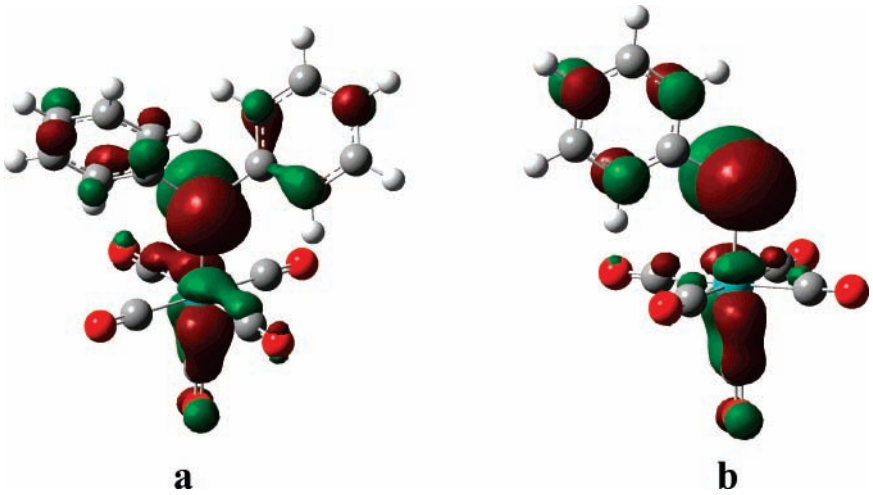

Figure 4. (a) SOMO for $Mo(CO)_5P(C_6H_5)_2$ and (b) LUMO for $Mo(CO)_5P(C_6H_5)$.

from those measured for isolated $Ph_2P^{\bullet}$ radicals by at least two features: (1) the ^{31}P isotropic coupling constants are almost twice as large as those for $Ph_2P^{\bullet}$, whereas the anisotropic coupling constants are appreciably smaller than those for the phosphinyl radical, and (2) the *g* anisotropy is more marked for the Mo and W complexes than for the isolated radical. Since the trapping properties are in good accord with the scission of a P−R bond (vide supra), these differences are due to the coordination of the phosphinyl type radical to the metal pentacarbonyl moiety, and indicate, therefore, the formation of the desired species $M(CO)_5PR_2$.

This conclusion is confirmed by DFT calculations which are well-known to accurately determine the dipolar hyperfine interactions. For almost all complexed radicals reported in Tables 4 and 6, the measured and calculated ^{31}P anisotropic coupling tensors present an axial symmetry and, taking a small dispersion of the experimental values due to the various environments (vide supra) into account, the accord between experimental and DFT values for the τ_{max} component is excellent. As often reported for phosphorus radicals, the predicted isotropic ^{31}P couplings are noticeably smaller than the experimental ones; nevertheless, it is worthwhile remarking that DFT predicts an increase of between 50% and 100% when passing from $P(C_6H_5)_2$ to $M(CO)_5P(C_6H_5)_2$ and that this change is consistent with the increase measured on the EPR spectra.

Finally, the *g*-eigenvalues calculated for $M(CO)_5PPh_2$ (M = Cr, Mo, W) reasonably agree with the experimental values reported in Table 3, inasmuch as the relative orientations of the *g* and ^{31}P hyperfine coupling correspond to the orientation determined from EPR measurements. The calculated *g*-tensors confirm that coordination of PPh_2 to $Mo(CO)_5$ and $W(CO)_5$ provokes an appreciable enhancement of the *g* anisotropy.

Since the properties calculated for $M(CO)_5PR_2$ (Table 6) are consistent with those measured by EPR, we can use DFT to describe the structure of complexed phosphinyl radicals. This structure is illustrated for $Mo(CO)_5P(C_6H_5)_2$ in Figure 4; the reference axes are defined in Figure 5. The lone pair of the sp^2-hybridized phosphorus atom forms a σ bond with the empty metal d_{z^2} orbital. The antibonding combination resulting from the interaction between the p_x phosphorus orbital oriented perpendicular to the CPC plane and the doubly occupied molybdenum d_{xz} orbital leads to the SOMO shown in Figure 4.

This SOMO corresponds, in fact, to the LUMO of the phosphinidene transition metal complex described by Nguyen.[35] We have optimized the structure of the phosphinidene $Mo(CO)_5$ complex with the functional and basis sets used for the

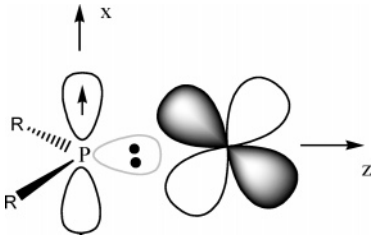

Figure 5. Relative orientation of the phosphinyl and metal moieties in $R_2PM(CO)_5$.

phosphinyl $Mo(CO)_5$ complex. The resulting LUMO is shown in Figure 4. By passing from the phosphinidene complex $M(CO)_5PR$ (singlet state) to $M(CO)_5PR_2$, one of the phosphorus lone pairs is replaced by a σ P−C bond and an unpaired electron occupies the vacant p_x orbital. For the three complexes $M(CO)_5P(C_6H_5)_2$ (M: Cr, Mo, W), the C−P−C bond angle is equal to ca. 107 ° and the P−M bond lies in the bisector of this angle. For both the molybdenum and the tungsten complexes, the ξ angle formed by the P−M bond and the normal to the two P−R bonds (Table 5) is equal to 90°, indicating that the CPC plane is perpendicular to the equatorial plane. Such a structure readily explains the differences in the EPR parameters that accompany the coordination of the diphenylphosphinyl radical to the molybdenum pentacarbonyl moiety.

The overlap between the phosphorus p_x orbital and the metal d_{xz} orbital delocalizes a small part of the spin onto the metal. This tends to enhance the *g* anisotropy and appreciably changes the ^{31}P hyperfine interaction: decrease in the dipolar coupling (from 519 MHz for $P(C_6H_5)_2$ to 453 MHz for $Mo(CO)_5P(C_6H_5)_2$) due to a diminution of the phosphorus p spin density and increase in the isotropic coupling A_{iso} (from 164 MHz to 281 MHz). This enhancement of A_{iso} is probably due to the presence of spin in the d_{xz} orbital, which polarizes the metal−phosphorus σ bond. Such a polarization, even though quite small, is expected to increase the Fermi interaction at the phosphorus nucleus since the corresponding σ orbital has a pronounced s character (formally a phosphorus sp^2 orbital).

This interpretation is also consistent with the results obtained for the chromium complex although, in this case, the metal atom does not exactly lie in the PCP plane.

It is worthwhile remarking that, as indicated by the experimental (Table 4) and calculated (Table 6) values, the phosphorus spin density for $M(CO)_5P(C_6H_5)_2$ hardly varies when going down in column 6 of the Periodic Table while the *g* anisotropy appreciably increases. This *g* variation is therefore mainly caused by an increase of the spin−orbit coupling constant.[36]

5. Conclusion

As confirmed by DFT calculations, complexes between phosphinyl radicals and transition metal pentacarbonyls could be stabilized, at room temperature, in crystalline matrices. They show that in $M(CO)_5P(C_6H_5)_2$ the unpaired electron mainly resides in a phosphorus p orbital, which is oriented parallel to the equatorial plane of the complex. The interaction between this orbital and a d_{xz} metal orbital leads to appreciable changes in the ^{31}P coupling tensors as compared to those measured or calculated on the isolated phosphinyl species. For the Mo and W complexes an increase in the *g* anisotropy is also detected. The mechanism used to rationalize these changes implies a small delocalization of the spin from the phosphorus p orbital to the metal d_{xz} orbital. Nevertheless, the main characteristics of the phosphinyl radicals are maintained, in accordance with structure **A** of Scheme 1 and a very small contribution of structure **C**.

Acknowledgment. We gratefully acknowledge support from the Swiss National Science Foundation.

Supporting Information Available: Experimental angular variations of the EPR spectra in the three reference planes for $Cr(CO)_5P(C_6H_5)_3$, $Cr(CO)_5P(H)(C_6H_5)_2$, $Mo(CO)_5P(C_6H_5)_3$, $W(CO)_5P(C_6H_5)_3$, and $W(CO)_5P(H)(C_6H_5)_2$ together with the angular dependences calculated with the tensors given in Table 2, optimized structures for $(C_6H_5)_2P^{\bullet}$, figures showing atom numbering and ellipsoids for the crystal structures, and crystallographic data in CIF format. This material is available free of charge via the Internet at http://pubs.acs.org.

References and Notes

(1) Limberg, C. *Angew. Chem., Int. Ed*. **2003**, *42*, 5932.

(2) Auclair, K.; Hu, Z.; Little, D. M.; Ortiz de Montellano, P. R.; Groves, J. T. *J. Am. Chem. Soc.* **2002**, *124*, 6020.

(3) The adjective "non-innocent" was first used by C. K. Jorgensen for ligands where the degree of electron donation is uncertain due to their π-acceptor character. Jorgensen, C. K. *Oxidation numbers and oxidation states*; Springer: Berlin, Germany, 1969.

(4) Breher, F.; Böhler, C.; Frison, G.; Harmer, J.; Liesum, L.; Schweiger, A.; Grützmacher, H. *Chem. Eur. J.* **2003**, *9*, 3859.

(5) Hetterscheid, D. G. H.; Kaiser, J.; Reijerse, E.; Peters, T. P. J.; Thewissen, S.; Blok, A. N. J.; Smits, J. M. M.; de Gelder, R.; de Bruin, B. *J. Am. Chem. Soc.* **2005**, *127*, 1895.

(6) MacAdams, L. A.; Buffone, G. P.; Incarvito, C. D.; Golen, J. A.; Rheingold, A. L.; Theopold, K. H. *Chem. Commun.* **2003**, *10*, 1164.

(7) Poli, R. *Chem. Rev.* **1996**, *96*, 2135.

(8) Büttner, T.; Geier, J.; Frison, G.; Harmer, J.; Calle, C.; Schweiger, A.; Schönberg, H.; Grützmacher, H. *Science* **2005**, *307*, 235.

(9) (a) Choua, S.; Sidorenkova, H.; Berclaz, T.; Geoffroy, M.; Rosa, P.; Mézailles, N.; Ricard, L.; Mathey, F.; Le Floch, P. *J. Am. Chem. Soc.* **2000**, *122*, 12227. (b) Cataldo, L.; Choua, S.; Berclaz, T.; Geoffroy, M.; Mézailles, N.; Avarvari, N.; Mathey, F.; Le Floch, P. *J. Phys. Chem. A* **2002**, *106*, 3017. (c) Jouaiti, A.; Geoffroy, M.; Terron, G.; Bernardinelli, G. *J. Am. Chem. Soc.* **1995**, *117*, 2251.

(10) Hou, Z.; Breen, T. L.; Stephan, D. W. *Organometallics* **1993**, *12*, 3158. Ho, J.; Rousseau, R.; Stephan, D. W. *Organometallics* **1994**, *13*, 1918.

(11) Planas, J. G.; Gladysz, J. A. *Inorg. Chem.* **2002**, *41*, 6947. Eichenseher, S.; Delacroix, O.; Kromm, K.; Hampel, F.; Gladysz, J. A. *Organometallics* **2005**, *24*, 245. Planas, J. G.; Hampel, F.; Gladysz, J. A. *Chem. Eur. J.* **2005**, *11*, 1402.

(12) Kato, Z.; Gornitzka, H.; Baceiredo, A.; Schoeller, W. W.; Bertrand, G. *J. Am. Chem. Soc.* **2002**, *124*, 2506. Dumitrescu, G. H.; Schoeller, W. W.; Bourissou, D.; Bertrand. G. *Eur. J. Inorg. Chem.* **2002**, 1953. Driess, M.; Muresan, N.; Merz, K.; Päch, M. *Angew. Chem., Int. Ed.* **2005**, *44*, 6734.

(13) Cowley, A. H.; Kemp, R. A. *Chem. Rev.* **1985**, *85*, 367. Nakazawa, H. *J. Organomet. Chem.* **2000**, *611*, 349. Gudat, D. *Coord. Chem. Rev.* **1997**, *163*, 71. Nakazawa, H. *Adv. Organomet. Chem.* **2004**, *50*, 107. Burck, S.; Daniels, J.; Gans-Eichler, T.; Gudat, D.; Nättinen, K.; Nieger, M. *Z. Anorg. Allg. Chem.* **2005**, *631*, 1403.

(14) Matthew, C. N.; Magee, T. A.; Wotiz, J. H. *J. Am. Chem. Soc.* **1959**, *81*, 2273.

(15) Marinetti, A.; Bauer, S.; Ricard, L.; Mathey, F. *Organometallics* **1990**, *9*, 793.

(16) Soulié, E. J.; Berclaz, T. *Appl. Magn. Reson.* **2005**. *29*, 401.

(17) Frisch, M. J.; Trucks, G. W.; Schlegel, H. B.; Scuseria, G. E.; Robb, M. A.; Cheeseman, J. R.; Montgomery, J. A., Jr.; Vreven, T.; Kudin, K. N.; Burant, J. C.; Millam, J. M.; Iyengar, S. S.; Tomasi, J.; Barone, V.; Mennucci, B.; Cossi, M.; Scalmani, G.; Rega, N.; Petersson, G. A.; Nakatsuji, H.; Hada, M.; Ehara, M.; Toyota, K.; Fukuda, R.; Hasegawa, J.; Ishida, M.; Nakajima, T.; Honda, Y.; Kitao, O.; Nakai, H.; Klene, M.; Li, X.; Knox, J. E.; Hratchian, H. P.; Cross, J. B.; Adamo, C.; Jaramillo, J.; Gomperts, R.; Stratmann, R. E.; Yazyev, O.; Austin, A. J.; Cammi, R.; Pomelli, C.; Ochterski, J. W.; Ayala, P. Y.; Morokuma, K.; Voth, G. A.; Salvador, P.; Dannenberg, J. J.; Zakrzewski, V. G.; Dapprich, S.; Daniels, A. D.; Strain, M. C.; Farkas, O.; Malick, D. K.; Rabuck, A. D.; Raghavachari, K.; Foresman, J. B.; Ortiz, J. V.; Cui, Q.; Baboul, A. G.; Clifford, S.; Cioslowski, J.; Stefanov, B. B.; Liu, G.; Liashenko, A.; Piskorz, P.; Komaromi, I.; Martin, R. L.; Fox, D. J.; Keith, T.; Al-Laham, M. A.; Peng, C. Y.; Nanayakkara, A; Challacombe, M.; Gill, P. M. W.; Johnson, B.; Chen, W.; Wong, M. W.; Gonzalez, C.; Pople, J. A. *Gaussian 03*, Revision B.03; Gaussian, Inc.: Pittsburgh, PA, 2003.

(18) Becke, A. D. *J. Chem. Phys.* **1993**, *98*, 6548.

(19) Lee, C.; Yang, W.; Parr, R. G. *Phys. Rev. B* **1988**, *37*, 785.

(20) (a) Stevens, W. J.; Krauss, M.; Basch, H.; Jasien, P. G. *Can. J. Chem.* **1992**, *70*, 612. (b) Stevens, W.; Basch, H.; Krauss, J. *J. Chem. Phys.* **1984**, *81*, 6026. (c) Cundari, T. R.; Stevens, W. J. *J. Chem. Phys.* **1993**, *98*, 5555.

(21) Basis set obtained from the Extensible Computational Chemistry Environment Basis Set Datababase, Version 02/25/04, as developed and distributed by the Molecular Science Computing Facility, Environmental and Molecular Sciences Laboratory, which is part of the Pacific Northwest Laboratory, P.O. Box 999, Richland, WA 99352.

(22) Kutzelnigg, W.; Fleischer, U.; Schindler, M. In *NMR−Basic Principles and Progress*; Springer-Verlag: Heidelberg, Germany, 1990; Vol. 23.

(23) (a) Godbout, N.; Salahub, D. R.; Andzelm, J.; Wimmer, E. *Can. J. Chem.* **1992**, *70*, 560. (b) Schäfer, A.; Horn, H.; Ahlrichs, H. *J. Chem. Phys.* **1992**, *97*, 2571. (c) Schäfer, A.; Huber, C.; Ahlrichs, *J. Chem. Phys.* **1994**, *100*, 5829.

(24) *GaussView 3.0*; Gaussian, Inc.: Pittsburgh, PA.

(25) Some references for the calculation of EPR properties. (a) *Calculation of NMR and EPR Parameters*; Kaupp, M., Bühl, M., Malkin, V. G., Eds.; Wiley-VCH: Weinheim, Germany, 2004. (b) Nguyen, M. T.; Creve, S.; Erikson, L. A.; Vanquickenborne, L. G. *Mol. Phys.* **1997**, *91*, 537. (c) Barone, V. In *Recent Advances in density Functional Methods*; Chong, D. P., Ed.; World Scientific: Singapore, 1995. (d) Patchkovskii, S.; Ziegler, T. *J. Am. Chem. Soc.* **2000**, *122*, 3506. (e) Van Lenthe, E.; Wormer, P. E. S.; van der Avoird, A. *J. Chem. Phys.* **1997**, *107*, 2488.)

(26) (a) Neese, F. *J. Chem. Phys.* **2001**, *115*, 11080. (b) Harriman, E. *Theoretical Foundations of Electron Spin Resonance*; Academic Press: New York, 1978. As an example of the application with free radicals see: Mattar, S. B. *Chem. Phys. Lett.* **2005**, *405*, 382.

(27) Cotton, F. A.; Darensbourg, D. J.; Isley, W. H. *Inorg. Chem.* **1981**, *20*, 578.

(28) Aroney, M. J.; Buys, I. E.; Davies, M. S.; Hambley, T. W. *J. Chem. Soc., Dalton Trans.* **1994**, 2827.

(29) Plastas, J. H.; Stewart, J. M.; Grim. S. O. *J. Am. Chem. Soc.* **1969**, *91*, 4326.

(30) It should be noted that for M = Mo[27] and Cr,[29] the published unit cells were not reduced. All EPR reference axes reported in the present article were defined from the reduced cells ($a < b < c$ and $\alpha, \beta, \gamma < 90°$).

(31) Daly. J. J. *J. Chem. Soc.* **1964**, 3799.

(32) The angular variations of the EPR spectra, in the three reference planes, for the five single crystals $Cr(CO)_5P(C_6H_5)_3$, $Cr(CO)_5P(H)(C_6H_5)_2$, $Mo(CO)_5P(C_6H_5)_3$, $W(CO)_5P(C_6H_5)_3$, and $W(CO)_5P(H)(C_6H_5)$ are given as the Supporting Information.

(33) Geoffroy, M.; Lucken, E. A. C.; Mazeline, C. *Mol. Phys.* **1974**, *28*, 839.

(34) Morton, J. R.; Preston, K. F. *J. Magn. Reson.* **1978**, *30*, 577.

(35) (a) Creve, S.; Pierloot, K.; Nguyen, M. T.; Vanquickborne, L. G. *Eur. J. Inorg. Chem.* **1999**, 107. (b) Creve, S.; Pierloot, K.; Nguyen, M. T. *Chem. Phys. Lett.* **1998**, *285*, 429.

(36) Some spin−orbit coupling constants (e.g., for Cr(I) 56 cm^{-1}, for Mo(I) 168 cm^{-1}, for W(I) 607 cm^{-1}) are compiled in: Fraga, S.; Karwowski, J.; Saxena, K. M. S. *Handbook of atomic data*; Elsevier: New York, 1976.